IJIE

The International Journal of Integrated Engineering

An Experimental Investigation on Converting Conventional to Supercharged CI Engine

Balaji Ganesh N.[1*], P. V. Sri Hari[1]

[1]R.V. College of Engineering, R V Vidyanikethan Post, Bengaluru, 560059, INDIA

*Corresponding Author

Abstract: Due to the increase in grounds performance of internal combustion engines, the diesel engine has become dominant forces in the power, propulsion, and energy. For domestic, industrial, and transportation applications, internal combustion engines are the more reliable and misogynist power source. Diesel engines rely on fluid Spritz dynamics for air-fuel mixtures and swirl plays a crucial role in the pattern of air motion as impacts fuel air mixing and combustion. Further-more, older studies have indicated that it affects heat transfer, combustion efficiency, and engine emissions. By varying air inlet pressure, this work demonstrates the presentation and production features of Compression Ignition engines. Using compressor, the inlet pressure of air is manipulated, and when compressed air is sent to engine at different pressures, performance parameters and heat balance sheets are calculated.

Keywords: CI engine, supercharging, air inlet pressure, air compression, four-stroke CI

1. Introduction

The invention of Compression Ignition (CI) engines and the subsequent changes of engine technology paved the vast spread of exploitation in petroleum reserves, which are quickly depleting [1]. Several research groups are investigating clean diesel engine technologies for passenger cars to meet stringent emission requirements and improve fuel efficiency. During the combustion and after the treatment, clean diesel engine technology approaches would be divided into combustion control. Biofuels are studied widely in CI engines to increase energy security and reduce greenhouse gas emissions [2][3]. There will be a significant impact on the economy's growth and poverty reduction worldwide. The former findings from the literature reviewed show that biodiesels have comparable power. Brake Specific Fuel Consumption (BSFC) and brake efficiency of thermal are used in engines compared to diesel engines [4]. Biodiesel significantly offers portability advantages, and many studies have shown higher combustion efficiency with biodiesel, although there is little consensus [5]. In addition, biodiesel provides low sulfur and aromatic content, high cetin number, and high lubricity [6]. Various parameters characterize the Efficiency of an Internal Combustion (IC) engine. Important parameters are specific braking fuel consumption, effective force, heat capacity, cylinder pressure and heat release rate [7,8,9]. Many researchers have studied biodiesel's performance characteristics and its blends-powered engines and compared them with traditional diesel engines [10; 11]. The operating characteristics of internal combustion engines are fueled by biodiesel blends [12]. Turbulent Kinetic Energy (TKE) [13] improves speed, swirl and swirling combustion, ultimately improving engine efficiency, and reducing emissions.

This work ensures that the procedures used by researchers worldwide ignore the effect of airflow in the cylinder and focus only on optimizing the fuel side [14; 15]. No research has attempted to improve in-cylinder airflow characteristics to improve engine performance and reduce emissions when operating in HVF. Because of this shortcoming, this study used a reference fleet to investigate the performance and emissions of biodiesel-fueled internal combustion engines [16]. Guide vanes were used to create structured turbulence in front of the inlet runner and were expected to improve TKE, velocity, vorticity, and vorticity. Hypothetically, it is suggested that this method improves

vaporization and dispersion, and in air, there are mixed injected biodiesel, theoretically improving the engine's performance and emissions that reduce [17]. This study shows that no research has been done to improve CI biodiesel cylinders' characteristics to solve the problems above [18]. Hypothetically, more turbulence would further break the molecular chains of the biodiesel and accelerate the rapid process of mixing [19]. This is predictable to improve the vaporizing, dispersing and mixing bio-diesel with air injection, leading to better performance and lower emissions in internal combustion engines. Therefore, the simulation results must be verified experimentally or compared with the work of other researchers [20]. Once the simulation results are confirmed in this study, it is likely needed that the research results can be straightly applied in the purification, which is required for biodiesel.

In this work, we implemented a spiral screw collector that creates a vortex when entering the cylinder. Turbulence is achieved by directing airflow through the intake manifold threads. Tests are performed using different configurations of spiral threads from the intake manifold. Measurements were performed with a speed of constant 1500 rpm. The results are related to normal and helical screw collectors. We implement the manifold with a nozzle for air velocity while incoming the tube. The turbulence was attained in the inlet various by inserting a convergent nozzle in the inlet manifold from 30 to 15mm diameter to direct the airflow. The tests are carried out with different configurations by placing a convergent nozzle of the manifold intake in its inlet. Also, capacities were done at a continuous speed of 1500 RPM. The fallouts are associated among nor-mal various and multiple with nozzle. The remaining of this work is prearranged as follows: Section 2 defines the current works connected to the supercharged CI engine. In Section 3, we deliberate the experimental setup and procedures of the present study. The working process of the proposed methodology is briefly discussed in Section 4. The untried fallouts and comparative analysis are illustrated in Section 5. The paper is decided in Section 6.

2. Related Works

Cha et al. [21] proposed an experimental study of combustion and emission characteristics of internal combustion engines at various equivalence ratios up to stoichiometric conditions. To control the equilibrium ratio, we reduced the O2 mole fraction of the injected gas from 21% to 11.16%, kept the injected fuel constant and added only N2 to the injected gas. The test used a 373.3 cc re-intake piston bowl CI engine with a compression ratio of 17.8. Kasiraman et al. [22] reported the successful start-up of a single-cylinder compression-ignition engine using pure cashew oil, diesel, and CNSO methyl ether. Then, experiments were conducted using CNSO with different combinations of oxygen, alcohol, and vegetable oil. These blends' performance and combustion characteristics are compared to all-electric source fuels. Based on the experimental results, the following conclusions are drawn.

Xiao et al. [23] compared the designs of RSCn-butanol/diesel and CSCn-butanol using a combination of KIVA-3V code and non-dominated genetic algorithm II (NSGA-II). For RCS and CSC, n-butane is supplied under the start port. Diesel and n-butanol are injected into the RSC and CSC cylinders, respectively. Five key performance parameters, including Premix Fraction (PF), Start of Injection (SOI), Initial Cylinder (IVC), initial valve closing time, initial cylinder temperature, IVC time and EGR ratio, were selected for optimization. The optimization results show that RSC uses a wide range of power factors and factors, while CSC uses a wide range of power factors and intrinsic Efficiency to achieve pure and high-power Efficiency. Li et al. [24] proposed direct injection using direct injection of high-pressure methane. Therefore, we conducted gas injection and combustion experiments with a single-cylinder CI engine with a compression ratio of 15.5. A multipoint GTI injector operating at various loads of 400 bars was used to raise the threshold temperature to 400°C to reach the compressed auto-injection methane temperature for fuel injection. Experiments were injected with times and injection pressures. Bhuya et al. [25] suggest that the engine speed varies between 1200 rpm and 2400 rpm at 200 rpm intervals. Performance characteristics of biodiesel blend like BP and BSFC increase with increasing engine speed at full load condition; BSFC has some exceptions at 1400 rpm; on the other hand, BTE and BMEP of biodiesel blend decrease with engine speed by 100%; load with the small exception of 1400rpm.

Hamid etc. [26] proposed a Guide Vane Design (GVD) that prioritizes the number of plates; 3 to 5 attempts are made to overcome the above problems of preloading the receiver manifolds. Emulsified Biofuel (EB) and GVD were manipulated with constant film height, angle and length to improve airflow characteristics in the cylinder; Proper diffusion improves evaporation and combustion. A 35° angled intake manifold radius, 0.2R barrel height and 4 wing triple lengths provide advantages in turbulent kinetic energy (TKE) and rotation rate. Muthuraman et al. suggested running the engine with pure biodiesel and blends. Additionally, Jatrophacarcus diesel and methanol super clean diesel blends were used to demonstrate the effect on overall engine performance using Fuel Consumption (BSFC) and Brake Thermal Efficiency (BTE). The results show that the specific fuel consumption varies by 14% for B100. Thermal properties of brakes B100 (24%) Jatropha (JOME) diesel fuel (24.5%) close to B30, higher than B1000 s.

Olanrewaju et al. [27] Proposed a 96 kW HRR model, modified with a multi-fuel injection, Euro V, direct injection (DI) engine. The modified HRR model estimated the engine fuel consumption of the CI engine with an average error of 1.41% compared to the accuracy of the HRR model. The typical estimation error for other models is 16%. More advanced HRR models lead to more accurate fuel consumption estimates that optimize and optimize better fuel consumption management strategies for engines and fuels. According to Akıntunde et al. [28] suggested that the use of fossil fuels in most combustion systems is inevitable as an important aspect of global development. This fuel type

contributes significantly to global environmental pollution, human health, and its effects on climate change. Bio-mass-derived biofuels are a sustainable and viable alternative that reduces the problems associated with petroleum fuels and is more compatible with combustion systems. Sanni, S.E. and more [29] suggested that the properties of waste tire/plastic-derived fuel were determined and compared with diesel fuel. Polyethylene terephthalate, polypropylene, high-density polyethylene, polystyrene, low-density polyethylene, poly and waste oil distilled from used Dunlop tires are used in varying amounts as alternative fuels CI engines. Engine performance was investigated regarding combustion, Brake Thermal Efficiency (BTE) and emission characteristics when operating with waste/plastic fuel.

3. Experimental Setup and Procedures

This chapter presents the details of the experimental setup and describes the modifications made to the instrument. As shown in Fig. 1, the experimental setup was designed to meet the goal of the work we process. This section presents the types of components, including the transformation of the test system.

3.1 Experimental Setup

This experiment system includes the engine, the spring balancing for the load on the engine, the fuel tank connected to the burette and a digital tachometer for checking the constant speed. KIRLOSKAR Company manufactured the engine, and it is a single cylinder upright type four-stroke, Water-cooled, compression ignition engine. The types and characteristics of self-driving vehicles used in this paper are given in Table 1. It is one of the most used engines in the industrial sector in India. This motor can withstand high compression due to its high compression ratio. Furthermore, the necessary modifications to the cylinder head and piston crown can easily be made in this engine type. So far, this engine has been specified for the current project. The loads at the engine were increased by using the spring balance readings, and those readings will be noted. The fuel consumption is un-rushed by the flask, which is having capacity of 100c.c. It is connected by three-way cocks so that fuel abounds to the machine through a burette. To measure the fuel, the engine consumes at various loads, time is taken against the fuel level drop in 10. c.c. To measure the fuel, close the stop cock and start the clock, and measure the time occupied for the ingesting of 10 cc of fuel.

Table 1 - Specification for the experimental setup

Engine Specification	Value
Make of the engine	Kirloskar AV1
Bore Diameter	88mm
Stroke Length	116mm
Compression ratio	16:1
Temperature	28ºC
Rated Output	5HP
Number of cylinders	One
General Details	Four-stroke CI engine with 1500rpm speed
Type of cylinder	Vertical cylinder
Cooling	Water-cooled standard engine
Type of fuel injection	Direct Injection
Starting	Hand start
Overall Dimensions of Engine	617×504×843(L×W×H)

The following parameters have been used to analyze the proposed methodology:
i. Quantity of time: Burette tube measures the fuel flow between the fuel pump and tank. A T-joint is made, and a fuel meter pipe is connected to one of its sides. The two sides remaining of the joint are connected to the fuel pump and fuel tank correspondingly. A stopwatch measures the time needed to consume 10 cc of fuel.
ii. Quantity of manometer readings: Manometer readings are measured using liquid flow in a U-tube manometer in the diesel test rig.
iii. Quantity of airflow: Airflow is unhurried using its velocity at the entrance of the intake manifold, and it was done using the anemometer. An anemometer consists of a fan whose speed of rotation indicates the velocity.
iv. Load on the engine: The engine will be ongoing, and it can run for 10 min to achieve a stable state disorder. The loading is applied in the stages of increasing loads.

Fig. 1 - View of the experimental setup with a four-stroke CI diesel engine

3.2 Experimental Procedure

Before the engine starts, check the lubricant state in the engine and also lubricate all moving and rotating parts. Then the engine starts and is allowed to run for 10 min until it stabilizes. The various steps involved in setting up tests are described below:

1. Tests are done after installing the device
2. The engine is started with no load and allowed to run for at least 10 min to get steady
3. Fuel consumption time, spring balance readings, manometer readings, cooling water flow rate and temperature are all taken per the observation schedule.
4. The load on the machine was increased using a spring balance, and measurements were taken, listed in the table.
5. Step 3 was repeated for different loads ranging from no load to full load
6. After the test, the engine loads are completely deducted, and the engine will be stopped.
7. By using the formulas, the results are to be calculated.

Here, overhead research was repetitive with different inlet air pressure. The untried process is comparable to the aforesaid. Before preliminary the engine, the air is compressed in a compress to a certain pressure. Then the outlet of the compress is opened. It flows to the engine's inlet by flowing through a moisture filter. Where it removes the moisture while preliminary the engine, the fuel tank is occupied up to its size. The machine runs for 10min for stable state circumstances, maintaining a constant flow of inlet of compressed air before the load is applied.
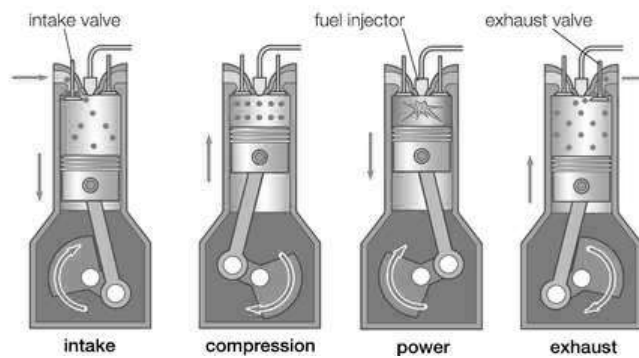

Fig. 2 - Various strokes of an engine

4. Discussion

4.1 Four-Stroke CI Engine

The cycle of operations is completed by crankshafts two revolutions (or) four strokes of the piston. The five events of intake, compression, combustion, expansion and exhaust must be completed in four strokes. Each stroke consists of 180 degrees of crankshaft rotation, so a four-stroke cycle is completed at 720 degrees. Because of the high compression ratio, the end temperature of the compression stroke is used to a high extent for the self-ignition of the combustion chamber with the fuel injected. Fig. 2 shows the sequence of operations for a four-stroke CI engine.

1. Suction stroke: Only air is removed during suction. During this collision, the intake valve opens, and the exhaust valve closes.
2. Compression stroke: During drying, the air is compressed in the nozzle. This shock causes both valves to close.

3. Expansion stroke: Fuel injection starts during the compression stroke. As the injection rate increases, the burner maintains constant pressure during its expansion due to the movement of the piston and increases its volume. Heat is added continuously under pressure. After fuel injection is complete (i.e., after shutdown), combustion products are released.
4. Exhaust stroke: The piston moving from BDC to TDC pushes the combustion products to the surface. During this stroke, the exhaust valve and the intake valve close.
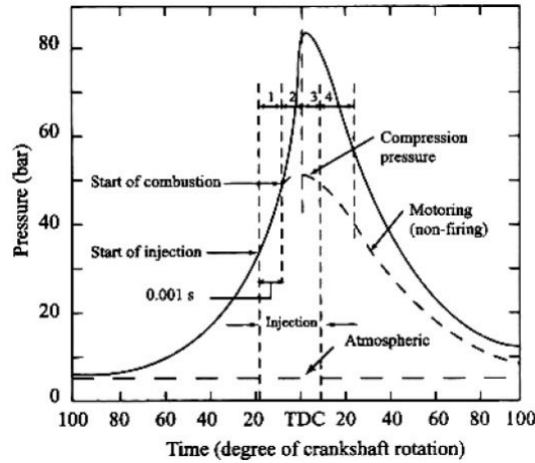

Fig. 3 - Combustion stages in CI engines

For SI engines, the A: F mixture is supplied, but for CI engines, the A: F mixture is not homogeneous, the fuel consists of liquid particles, so the amount of air supplied is 50-70% of that of the mixture. In an SI engine, combustion starts from a single point, and the flames generated during the combustion phase propagate through the mixture, igniting; Combustion occurs with several points simultaneously in the IC engine, and the number of batches produced is large. Because they exhale moisture, they are harder to burn; They must reach their ignition and thus exit. Fig. 3 shows the combustion running in the gun and explains how to create the sweet spot in four steps.

1. Ignition delay period /Pre-flame combustion
2. Uncontrolled combustion
3. Controlled combustion
4. After burning

Fuel does not burn immediately after entering the combustion chamber. There is an idle time between the injection time and the actual ignition time, called the ignition delay time. CI engine downtime greatly affects engine design and performance. This is especially important because of the combustion rate, knocking, starting the engine and the presence of exhaust fumes. The herd's rapid period, even as a fugitive burn, is when the pressure increases rapidly. During the delay, a significant amount of fuel accumulates in the combustion chamber, and these accumulated droplets ignite very quickly, causing rapid bursts in pressure. The duration of the rapid-fire is calculated from the time of the end delay of the device diagram or the maximum pressure at the beginning of the combustion. Currently, there is a high heat emission. It is also called runaway combustion because it is difficult to control the combustion /injection force during combustion. The effect of rapid ignition timing depends on the length of the delay.
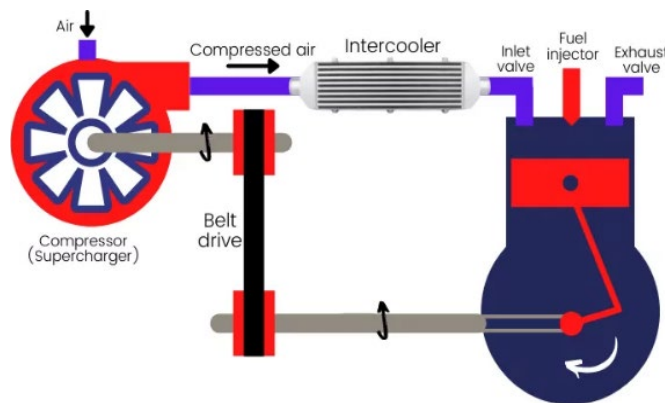

Fig. 4 - Schematic view of the supercharger

A rapid-fire phase is followed by a third phase, the command to burn. When the temperature and pressure are very high in the second stage, the injected fuel drops are almost burning to find the required oxygen, and the injection rate can control the increase in pressure. The combustion temperature is considered the maximum phase of the cycle. After the infusion process is complete, the combustion does not stop. When the first burnt and partially burnt parts of the fuel in the combustion chamber begin to encounter oxygen, they begin to burn. After some time, this process is called the adaptation phase. This sticking can resume when the throttle is advanced to 70-80% TDC. Latent time is between the start of injection and the start of combustion. The delay time spans about 13 degrees of arm rotation. This time delay decreases with increasing speed. The delay time should be as short as possible because a long delay causes a sudden increase in pressure, causing an explosion. Increasing or exceeding the pipe pressure automatically lowers the ignition temperature and thus reduces the delay time. The maximum pressure is higher because the pressure increases with the inlet pressure.

4.2 Supercharger

Superchargers (compressors) are pressure-boosting devices that increase the air pressure before entering the cylinder of an internal combustion engine. Increasing pressure or forcing more air into the engine is called supercharging. The general structure of a supercharger is shown in Fig. 4. A requirement in aircraft design is always high-power density, which means a small size and a high power-to-weight ratio. The reciprocating internal combustion engine was the first power source that met these requirements. When he did that, the developer was powerful and dominated that application until the 1940s. Today, besides being used in small aircraft, it has been surpassed by the gas turbine, which provides a higher energy density than a turbine propeller. The class of train engine used for this application was the 2-, 3- and 4-cylinder reciprocating steam engine. Today, diesel engine design is dominated by high-powered diesel engines with hydraulic or electric transmissions. Gas turbines have often been tested as a short-term power plant for this application but have failed due to energy efficiency and durability issues. We see how the internal combustion engine can handle small, decentralized, or small-scale power plants. Gas turbines are increasingly important for these applications to meet peak power requirements. Additionally, improvements over the past decade have reduced emissions while increasing productivity.

For commercial vehicle engines, turbocharging and charge air cooling contribute greatly to both sides. From heavy-duty trucks to dump trucks weighing about 4 tons, the turbocharged, air-cooled, direct-injection diesel engine is the only engine currently used in practice. Even in passenger cars, this engineering configuration stands out for its excellent performance. Regarding superchargers, gasoline passenger car engines continue to have problems due to high exhaust gas temperatures and the need for acceptable performance. The history of supercharged internal combustion engines goes back to Rudolf Diesel. Supercharged gasoline engines are obsolete at high speed. This uses the bottom of the piston to act as a mixture pump in a dual-duty four-stroke engine cycle, providing an additional mixture to the operating cylinder. The filling of the frame cavity is transmitted to the working cylinder through a valve located under the piston. The bold design was born from the desire to increase the speed and power of the engines, even though the intake and exhaust valves were too low. Supercharging was first widely used in aircraft engines, especially for high-altitude performance. From the 1920s to the 1940s, superchargers improved in aerodynamics and peripheral wheel speed. Gasoline engine refueling first peaked during World War II due to the power of aircraft engines and high performance. The turbocharger mechanically manages an average effective brake pressure of up to 23 bar.

4.3 Compressor

Air compressor systems provide small amounts of high-pressure compressed air for industrial and home use. It has become an indispensable tool in almost all fields. High Efficiency, possible operating parameters and various applications make the industry impossible without a compact compressor system. The main objective of this report is to understand the importance of air compressor systems. Furthermore, the report covers several compressor applications. The types of compressors, their advantages and their disadvantages are the same. Critical operating parameters and their importance in the compaction process are defined. It is rightly said that producing compressed air under high pressure is not economical and energy efficient. The report details some measures to reduce energy consumption and improve overall Efficiency. To understand the use of the compressor, a practical study of the operation of the ELGI compressor was carried out in the case of the Arab industry. Air compressors are classified as positive or dynamic depending on their internal mechanisms. The four most common air compressors are listed below.

1. Rotary screw compressor
2. Reciprocating air compressor (as shown in Fig. 5)
3. Axial compressor
4. Centrifugal compressor

Three intake manifolds (Fig. 6) are prepared in the present work. One is a normal manifold; the second is by providing internal threads inside the manifold; the last is placing a nozzle inside the manifold.

Fig. 5 - Reciprocating air compressor

Fig. 6 - Compressor outlet valve

4.4 Moisture Filters

Did you know that moisture is always present in atmospheric air? Even if we can't see when air is trodden in a beaten air system and cooled below its dew point, it condenses into liquid water. This creates a dilemma because compressed air systems rely on dry air and cannot perform their functions properly if the air is moist. In particular, the air must be free of liquid moisture, and the relative humidity must be below 50% to prevent corrosion. Want to know exactly what problems liquid water can cause in an air circuit? Check the following:

 i. It may block control airlines, interfere with gadget readings or proper processes, and cause general equipment malfunction.
 ii. By preventing lubrication, it will injure the air tools.
 iii. It damages pipes and apparatus, which causes water hammer events.
 iv. It damages the product and negates the integrity of the product; and
 v. Water entrainment from the air stream can directly affect the processes.

Removing moisture is important to protect equipment using air and air systems from corrosion. Odors and rust, and scale particles corrode air system components. Air is usually cooled upon entering the system, so it is most efficient to dehumidify the air before placing it in the air trap. Below are five ways to remove moisture from compressed air:

1. Cooling and separation are like this. The hot compressed air is cooled and allowed to condense large amounts of water. After condensation, the water could be taken from the air. This is usually followed by an after-cooler or heat exchanger that cools the hot compressed air and condenses the condensed water.
2. Compressing air to a higher pressure than intended for work is over-compression; after the separation, the air explodes to working pressure so that it would be used in the wanted process. Because this process will be energy intensive, high compression ratios is only appropriate for very small airflows.
3. Membrane drying uses a process that selects the gaseous components of air to separate the water vapor. When filtering, moist compressed air enters the cylinder, and the vapor penetrates the membrane coating and collects in the filaments; At the same time, dry air remains in the threads.
4. Absorption drying is a chemical process where steam is combined with an absorbent material such as sodium chloride/sulfuric acid. Absorbent materials can be solid or liquid and are less expensive than other drying methods.
5. Absorption drying involves the flow of moist air around hygroscopic materials for drying. Commonly used materials are silica gel, molecular sieves, activated alumina, regenerative absorption dryers, regenerative thermal washer dryers, regenerative air dryers, and heat screen dryers.

Weigh to the nearest 0.0001 g a vial of the indicated amount of sample moisture. Place the container and lid in a vacuum oven operated at a specified temperature and pressure for a specified time. One of these dishes is used as a blank, and the others are used for samples. Place the mixture in the sample container without the wires. Place the dishes in a vacuum oven at 100 degrees Celsius and a pressure of more than 25 torr. While the dish is drying, vent a small amount of air through the oven and drying rack. After 5 hours, close the vacuum and slowly fill the oven with air through the drying train. Open the oven, quickly cover the sample dishes and blanks, place in a desiccator, and cool to room temperature. Cover the sample containers and blanks for some time before weighing. Enter the weight to the nearest milligram. Accurately weigh 7 to 10 g of sample into a 45 mL (40x50 mm) volumetric flask. Add 10 ml of hot distilled water and mix well with a small glass rod. Pour the diluted sample into the sample container on the filter aid and complete the volume change of the sample with three 5 ml hot distilled water. Insert the steel extension rod into the weed tube in the sample vessel and stir until the sample is uniformly dispersed on the filter support.

Fig. 7 - View of simple moisture filter

Remove the handle, leave the mixing tube in the container, and place the empty beaker and sample cup in a vacuum oven set at 70°C for corn syrup above 58D.E. 100°C 58D.E for corn syrup. Filters play an important role in the compressed air supply process. Depending on the end use, strict hygiene standards require the removal of various contaminants, including oil aerosols and particulate matter. Contamination can enter compressed air from a variety of sources. Dust or particles can enter the incoming air, and corroded pipes can add harmful particles to the compressor system. Oil aerosols and vapors are often a byproduct of oil compressor use and must be filtered before final use. Fig. 7 shows a view of the moisture filter. Different compressed air applications have specific purity requirements, but the presence of impurities can exceed acceptable levels, causing reduced production or hazardous air. Filters are divided into three categories: consolidation, vapor removal, and dry particulate filters. While each type produces the same result, each works on different principles.

4.5 Numerical Formulae for Performance Analysis

Performance Parameters of I.C. Engines are calculated with the standard Mechanical Formulae. The Formulae for calculating various performance parameters are listed below; with the help of this, all the efficiencies are calculated and listed in Tables 2,3,4,5 and 6.

$$Load = Net \ X \ 9.81N \tag{1}$$

$$\text{Torque= Load × Torque Arm Length N-m,} \tag{2}$$

$$Brake \ Power \ (B.P) = \frac{2\pi nt}{60000} \ \text{Kw} \tag{3}$$

$$where, N = speed \ in \ RPM, t = Torqe \ in \ N-m$$

$$Total \ Fuel \ Consumption \ (TFC) = \frac{10}{T} X \frac{3600}{1000} X \ S.Fuel \ kg/Hr \tag{4}$$

where, t- Time occupied for 10c.c. of fuel, seconds

$$Brake - Specific \ Fuel \ Consumption \ (BSFC) = \frac{T.F.C}{B.P} \text{kg/Kwhr} \tag{5}$$

$$Heat \ Input = Mass \ of \ fuel \ X \ C.V \ kW = \text{T.F.C x C.V kW} \tag{6}$$

$$\text{where } C.V - \text{ Calorific value of fuel}, kJ/KG (42,000 \ kJ/kg)$$

$$\text{Mass of fuel} = \frac{10 \ X \ S.Fuel}{T \ X \ 1000} Kg/S \tag{7}$$

Frictional Power (F.R) kW (from the graph by William's line method) $\tag{8}$

$$\text{Indicated Power } (I.P) = b.p + f.p \ kW \tag{9}$$

$$\text{Mechnical Efficiency}, \ \eta_{\text{mech}} = \frac{b.p}{I.P} X \ 100\% \tag{10}$$

$$\text{Indicated thermal efficiency}, \eta_{\text{ith}} = \frac{I.P}{Heat \ input} X \ 100\% \tag{11}$$

$$\text{Brake Mean Effective Pressure}, B_{\text{mep}} = \frac{b.p \times 60}{l \times a \times N \times K} KN/m^2 \tag{12}$$

$$\text{where L} - \text{ length of the stroke } = 116mm,$$

$$\text{n} - \text{ number of power strokes } = \frac{1500}{2},$$

$$\text{A} - \text{ Area of the cylinder,}$$

$$\text{k} - \text{ no. of cylinders}$$

$$\text{Indicative Mean Effective Pressure}, i_{\text{mep}} = \frac{i.p \times 60}{l \times a \times N \times K} KN/m^2 \tag{13}$$

$$\text{Volumetric Efficiency}, \eta_{\text{vol}} = \frac{\text{Actual volume flow rate of air}}{\text{Theoretical Volume flow rate of air}} \times 100 \ \% \tag{14}$$

$$\text{Actual volume flow rate of air}(q_{\text{act}}) = c_d \times A \times \sqrt{2gh} am^3/s \tag{15}$$

$$\text{Co-efficient of discharge}(C_d) = 0.62; Area(A) = \frac{\pi d^2}{4} m^2; d = 0.02m \tag{16}$$

$$\text{Atmospheric airhead } (h_a) = h_w \times \frac{density \ of \ water}{density \ of \ air} \tag{17}$$

$$\text{The theoretical volume flow rate of air } (q_{\text{the}}) = \frac{\pi \times d^2 \times l \times n}{4 \times 60 \times 2} m^3/s \tag{18}$$

$$\text{where d- 0.08m; L- Stroke length 0.11m; N- Speed in RPM}$$

4.6 Numerical Formulae for Heat Balance Sheet Analysis

The heat Balance sheet provides the accountability of how much amount of heat is supplied during combustion and how much amount of heat is utilized to develop power during power stroke; remaining heat losses also calculated using the heat balance sheet for these standard formulae for measuring heat balance is given below with the heat balance sheet analysis is done and shown in Table 7,8,9,10 and 11.

$$\text{Load Applied} = Spring \ Balance \ Reading \times 9.81N \tag{19}$$

$$\text{Torque}(t) = Load \ Applied \times Torque \ Arm \ Length \ Nm \tag{20}$$

$$\text{Brackepower}(B.P) = \frac{2\prod NT}{60000} KW \tag{21}$$

$$\text{Total Fuel Consumtion}(TFC) = \frac{10}{t} \times \frac{3600}{1000} \times S_{fuel} in kg/hr \tag{22}$$

$$\text{Heat Input} = a = mr * Calorific \ value \ in \ kj/min \tag{23}$$

$$\text{Heat utilized for B.P} = \frac{2\prod NT}{60000} KJ/min \tag{24}$$

$$\text{Heat carried away by cooling water} = m_{wc} * c_{pw}(t_3 - t_2) KJ/min \tag{25}$$

$$\text{Heat carried away by exhaust gases} = mg * cpg(t_5 - t_1) \tag{26}$$

$$\text{where}, mg = mass \ of \ exhaust \ gases \ in \ kg/min = ma + mf$$

$$ma = Mass \ of \ air = Density \ of \ air \times c_d \times A \times \sqrt{2gH} \times 60 kg/min \tag{27}$$

$$\text{Unacounated lossese} = a - (b + c + d) \tag{28}$$

5. Experimental Results and Discussion

The results obtained from the experimental investigations on the performance using supercharging arrangement (reciprocating high inlet compressed and moisture filter) and discussed in the section are compressed with infinite inlet air pressure.

5.1 Comparative Analysis of CI Engine Performance Parameters

Here, we analyze the act of the CI engine with respect to different loads such as 1, 3, 5, 7 and 9 kg. Tables 2 to 6 describe the comparative analysis of CI engine performance parameters with respect to varying bar pressures 1, 2, 3, 4 and 5, respectively. Fig. 8 describes the comparative analysis of total fuel consumption with different bar pressures 1, 2, 3, 4 and 5. The total fuel consumption of bar-1 pressure is 4.403%, 8.74%, 13.042% and 17.117% higher than the bar-2, bar-3, bar-4, and bar-5 pressure respectively. The variation of total specific fuel consumption with load is shown in the plot; from the graph, total Fuel Consumption for all loads decreases gradually from normal cases to the 5-bar inlet pressure of air. Fig. 9 describes the comparative analysis of specified fuel consumption with different bar pressures 1, 2, 3, 4 and 5. The specified fuel consumption of bar-1 pressure is 2.536%, 3.119%, 7.999%, and 10.18% higher than the bar-2, bar-3, bar-4, and bar-5 pressure respectively. The variation of specific fuel consumption with load is shown in the plot. From this plot, specific fuel consumption for all the loads decreases gradually from normal cases to 5 bar inlet air pressure. Fig. 10 describes the comparative analysis of thermal brake efficiency with different bar pressures 1, 2, 3, 4 and 5. The brake thermal efficiency of bar-3 pressure is 45.544%, 7.155%, 36.731%, and 33.444% higher than the bar-1, bar-2, bar-4, and bar-5 pressure respectively. The variation of specific fuel consumption with load is shown in the plot. From this plot, specific fuel consumption for all the loads decreases gradually from normal cases to 5 bar inlet air pressure.
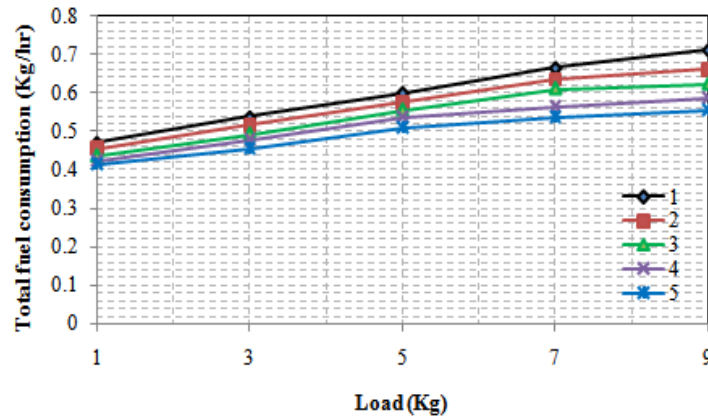

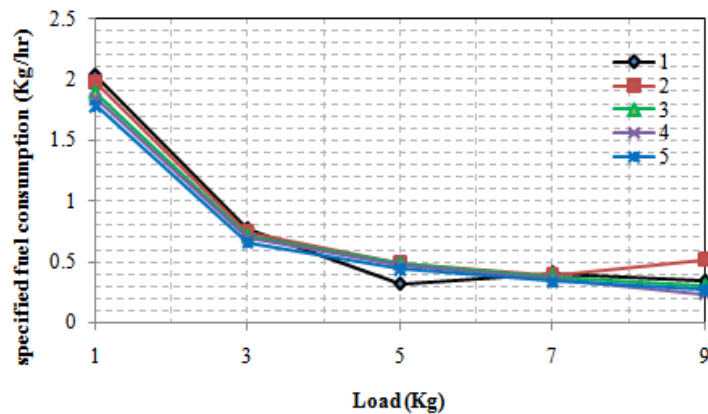Fig. 8 - Comparative analysis of total fuel consumption with different load

Fig. 9 - Comparative analysis of specified fuel consumption with different load
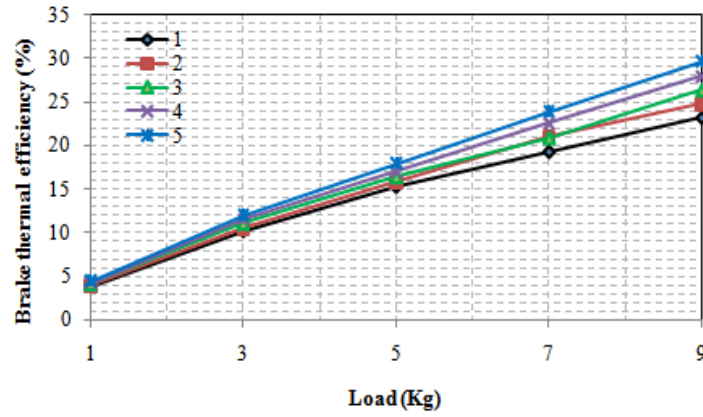
Fig. 10 - Comparative analysis of brake thermal efficiency with different load

Table 1 - Experimental results with 1-bar

S. No.	Description	Units	Trail 1	Trail 2	Trail 3	Trail 4	Trail 5
1.	Spring balance reading 1	Kg	0	0	0	0	0
2.	Spring balance reading 2	Kg	1	3	5	7	9
3.	Load	Kg	1	3	5	7	9
4.	Speed	RPM	1500	1500	1500	1500	1500
5.	Manometer readings	Mm	50	50	50	50	50
6.	Temperature (T1)	C	23	23	23	23	23
7.	Temperature (T2)	C	23	23	23	23	23
8.	Temperature (T3)	C	31	34	35	36	37
9.	Temperature (T4)	C	34	37	39	40	41
10.	Temperature (T5)	C	182	220	231	279	286
11.	Temperature (T6)	C	66	88	10	110	121
12.	Time taken for 10cc fuel	Sec	65	57	51	46	43
13.	Brake power	Kw	0.2311	0.6938	1.1557	1.6179	2.0802
14.	Total fuel consumption	Kg/hr	0.4707	0.5368	0.6000	0.665	0.7116
15.	Spec Fuel consumption	Kg/kWhr	2.037	0.774	0.319	0.411	0.342
16.	Heat input	Kw	5.915	0.7795	7.553	8.372	8.9635
17.	Friction power	Kw	0.75	0.75	0.75	0.75	0.75
18.	Medicated power	Kw	0.981	1.443	1.905	2.368	2.830
19.	Mechanical Efficiency	%	23.5	48	60	68.3	73.5
20.	Brake thermal Efficiency	%	3.9	10.22	15.3	19.3	23.2
21.	Indi. Thermal Efficiency	%	16.5	21.2	25.22	28.2	31.5
22.	Actual air intake (Q_{act})	m³/s	0.00537	0.00537	0.00537	0.00537	0.00537
23.	Theoretical air intake (Q_{The})	m³/s	0.00691	0.00691	0.00691	0.00691	0.00691
24.	Volumetric Efficiency	%	77.65	77.65	77.65	77.65	77.65
25.	B_{MEP}	kN/m²	33.615	100.838	168.101	235.33	302.57
26.	I_{MEP}	kN/m²	142.57	209.89	277.09	344.63	411.63

Table 2 - Experimental results with 2-bar

S. No.	Description	Units	Trail				
			1	2	3	4	5
1.	Spring balance reading 1	Kg	0	0	0	0	0
2.	Spring balance reading 2	Kg	1	3	5	7	9
3.	Load	Kg	1	3	5	7	9
4.	Speed	RPM	1500	1500	1500	1500	1500
5.	Manometer readings	Mm	50	50	50	50	50
6.	Temperature (T1)	C	23	23	23	23	23
7.	Temperature (T2)	C	23	23	23	23	23
8.	Temperature (T3)	C	38	38	38	39	39
9.	Temperature (T4)	C	41	42	43	43	44
10.	Temperature (T5)	C	203	225	240	239	274
11.	Temperature (T6)	C	96	103	108	115	121
12.	Time taken for 10cc fuel	Sec	65	57	51	46	43
13.	Brake power	Kw	0.2311	0.6938	1.1557	1.6179	2.0802
14.	Total fuel consumption	Kg/hr	0.4567	0.5180	0.5773	0.6375	0.6632
15.	Spec Fuel consumption	Kg/kWhr	1.9762	0.7474	0.4995	0.3940	0.5197
16.	Heat input	Kw	3.770	6.554	7.293	7.583	8.341
17.	Friction power	Kw	0.8	0.8	0.8	0.8	0.8
18.	Medicated power	Kw	1.0311	1.496	1.577	2.4179	2.8802
19.	Mechanical Efficiency	%	22.41	46.45	59.09	66.91	72.72
20.	Brake thermal Efficiency	%	4	10.58	15.85	20.99	24.76
21.	Indi. Thermal Efficiency	%	17.87	22.8	26.82	30.30	34.28
22.	Actual air intake (Q_{act})	m^3/s	0.0054	0.0054	0.0054	0.0054	0.0054
23.	Theoretical air intake (Q_{The})	m^3/s	0.0069	0.0069	0.0069	0.0069	0.0069
24.	Volumetric Efficiency	%	77.65	77.65	77.65	77.65	77.65
25.	B_{MEP}	kN/m^2	33.615	100.86	168.11	235.33	302.57
26.	I_{MEP}	kN/m^2	149.96	217.22	284.46	350	418.92

Table 3 - Experimental results with 3-bar

S. No.	Description	Units	Trail				
			1	2	3	4	5
1.	Spring balance reading 1	Kg	0	0	0	0	0
2.	Spring balance reading 2	Kg	1	3	5	7	9
3.	Load	Kg	1	3	5	7	9
4.	Speed	RPM	1500	1500	1500	1500	1500
5.	Manometer readings	Mm	50	50	50	50	50
6.	Temperature (T1)	C	23	23	23	23	23
7.	Temperature (T2)	C	23	23	23	23	23
8.	Temperature (T3)	C	37	38	38	39	39
9.	Temperature (T4)	C	39	40	42	43	44
10.	Temperature (T5)	C	214	227	253	276	333
11.	Temperature (T6)	C	100	103	108	115	121

			1	2	3	4	5
12.	Time taken for 10cc fuel	Sec	65	57	51	46	43
13.	Brake power	Kw	0.2311	0.6938	1.1557	1.6179	2.0802
14.	Total fuel consumption	Kg/hr	0.4371	0.4935	0.5563	0.612	0.6244
15.	Spec Fuel consumption	Kg/kWhr	1.8913	0.711	0.4813	0.3782	0.3001
16.	Heat input	Kw	5.5244	6.2373	7.031	7.735	7.891
17.	Friction power	Kw	0.72	0.72	0.72	0.72	0.72
18.	Medicated power	Kw	0.9511	1.4138	1.8757	2.3379	2.8002
19.	Mechanical Efficiency	%	24.29	49.07	61.61	69.20	74.28
20.	Brake thermal Efficiency	%	4.18	11.11	16.43	20.91	26.36
21.	Indi. Thermal Efficiency	%	17.21	22.66	26.27	30.22	35.48
22.	Actual air intake (Q_{act})	m³/s	0.0054	0.0054	0.0054	0.0054	0.0054
23.	Theoretical air intake (Q_{The})	m³/s	0.0069	0.0069	0.0069	0.0069	0.0069
24.	Volumetric Efficiency	%	77.65	77.65	77.65	77.65	77.65
25.	B_{MEP}	kN/m²	33.615	100.86	168.11	235.33	302.57
26.	I_{MEP}	kN/m²	138.34	205.64	272.82	340.04	407.3

Table 4 - Experimental results with 4-bar

S. No.	Description	Units	Trail				
			1	2	3	4	5
1.	Spring balance reading 1	Kg	0	0	0	0	0
2.	Spring balance reading 2	Kg	1	3	5	7	9
3.	Load	Kg	1	3	5	7	9
4.	Speed	RPM	1500	1500	1500	1500	1500
5.	Manometer readings	Mm	50	50	50	50	50
6.	Temperature (T1)	C	23	23	23	23	23
7.	Temperature (T2)	C	23	23	23	23	23
8.	Temperature (T3)	C	37	38	38	38	38
9.	Temperature (T4)	C	40	42	43	43	44
10.	Temperature (T5)	C	199	238	249	261	293
11.	Temperature (T6)	C	101	105	110	114	124
12.	Time taken for 10cc fuel	Sec	65	57	51	46	43
13.	Brake power	Kw	0.2311	0.6938	1.1557	1.6179	2.0802
14.	Total fuel consumption	Kg/hr	0.425	0.4781	0.5368	0.5666	0.5884
15.	Spec Fuel consumption	Kg/kWhr	1.839	0.689	0.4644	0.3502	0.2298
16.	Heat input	Kw	5.369	6.006	6.77	7.14	7.43
17.	Friction power	Kw	0.45	0.45	0.45	0.45	0.45
18.	Medicated power	Kw	0.6811	1.1438	1.6057	2.0679	2.5302
19.	Mechanical Efficiency	%	33.93	60.65	71.97	78.23	82.21

S. No.	Description	Units					
20.	Brake thermal Efficiency	%	4.30	11.55	17.07	22.65	27.99
21.	Indi. Thermal Efficiency	%	12.68	19.04	23.71	28.96	34.05
22.	Actual air intake (Q_{act})	m³/s	0.0054	0.0054	0.0054	0.0054	0.0054
23.	Theoretical air intake (Q_{The})	m³/s	0.0069	0.0069	0.0069	0.0069	0.0069
24.	Volumetric Efficiency	%	77.65	77.65	77.65	77.65	77.65
25.	B_{MEP}	kN/m²	33.615	100.85	168.10	235.33	302.57
26.	I_{MEP}	kN/m²	99.06	166.36	233.54	300.78	368.02

Table 5 - Experimental results with 5-bar

| S. No.	Description	Units	Trail				
			1	2	3	4	5
1.	Spring balance reading 1	Kg	0	0	0	0	0
2.	Spring balance reading 2	Kg	1	3	5	7	9
3.	Load	Kg	1	3	5	7	9
4.	Speed	RPM	1500	1500	1500	1500	1500
5.	Manometer readings	Mm	50	50	50	50	50
6.	Temperature (T1)	C	23	23	23	23	23
7.	Temperature (T2)	C	23	23	23	23	23
8.	Temperature (T3)	C	38	38	39	39	39
9.	Temperature (T4)	C	42	43	43	44	44
10.	Temperature (T5)	C	223	236	262	283	305
11.	Temperature (T6)	C	101	105	110	114	124
12.	Time taken for 10cc fuel	Sec	65	57	51	46	43
13.	Brake power	Kw	0.2311	0.6938	1.1557	1.6179	2.0802
14.	Total fuel consumption	Kg/hr	0.4135	0.4567	0.51	0.5368	0.5563
15.	Spec Fuel consumption	Kg/kWhr	1.7892	0.6582	0.4412	0.3317	0.2674
16.	Heat input	Kw	5.223	5.7694	6.44	6.7840	7.007
17.	Friction power	Kw	NA	NA	NA	NA	NA
18.	Medicated power	Kw	0.7311	1.1938	1.6557	2.1179	2.5802
19.	Mechanical Efficiency	%	31.60	58.11	69.8	76.39	80.6
20.	Brake thermal Efficiency	%	4.42	12.02	17.94	23.84	29.68
21.	Indi. Thermal Efficiency	%	13.99	20.69	25.70	31.21	36.82
22.	Actual air intake (Q_{act})	m³/s	0.0054	0.0054	0.0054	0.0054	0.0054
23.	Theoretical air intake (Q_{The})	m³/s	0.0069	0.0069	0.0069	0.0069	0.0069
24.	Volumetric Efficiency	%	77.65	77.65	77.65	77.65	77.65
25.	B_{MEP}	kN/m²	33.615	100.85	168.10	235.33	302.57
26.	I_{MEP}	kN/m²	106.34	172.42	240.82	308.04	375.3
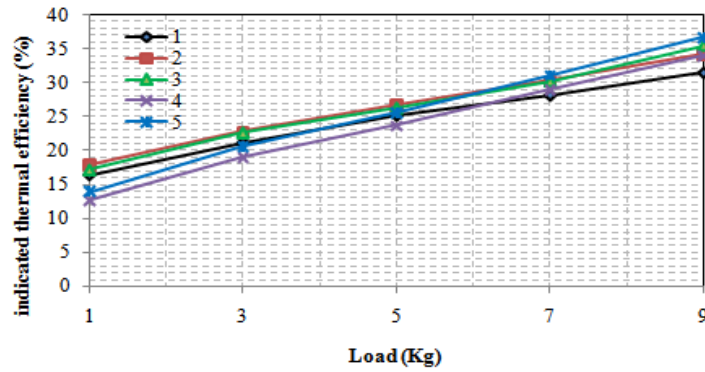
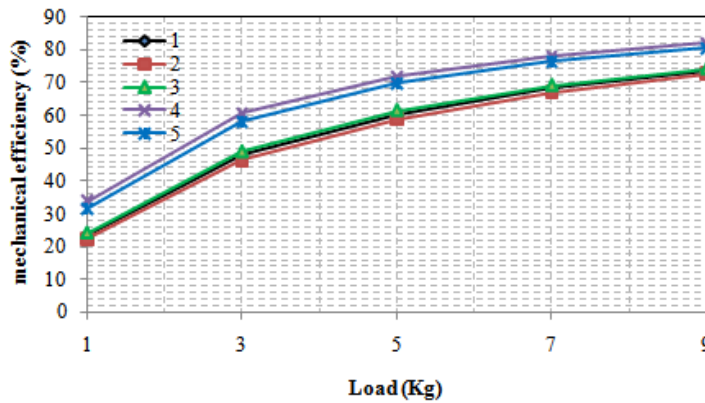**Fig. 1 - Comparative analysis of indicated thermal efficiency with different load**

Fig. 2 - Comparative analysis of mechanical efficiency with different load

Fig. **1** describes the comparative analysis of indicated thermal Efficiency with different bar pressures 1, 2, 3, 4 and 5. The indicated thermal efficiency of bar-2 pressure is 7.155%, 0.174%, 10.32% and 2.771% higher than the bar-1, bar-3, bar-4, and bar-5 pressure respectively. The variation of specific fuel consumption with load is shown in the plot. The graph shows the variation of brake thermal Efficiency with load for wearing inlet pressures of air in which air entering with the pressure of 5 bar has more brake thermal Efficiency when compared to that of remaining cases.

Fig. **2** describes a comparative analysis of mechanical Efficiency with the different bar pressures 1, 2, 3, 4 and 5. The mechanical efficiency respectively of bar-4 pressure is 16.419%, 18.169%, 14.844%, and 3.208% higher than the bar-1, bar-2, bar-3, and bar-5 pressure respectively. The variation of specific fuel consumption with load is shown in the plot. The variation of mechanical Efficiency with the load is shown in the plot; from this, mechanical Efficiency for all the loads increases gradually from normal cases to 5bar inlet pressure of air.
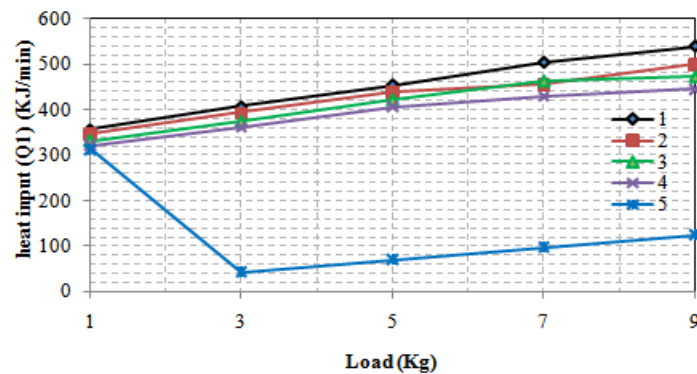

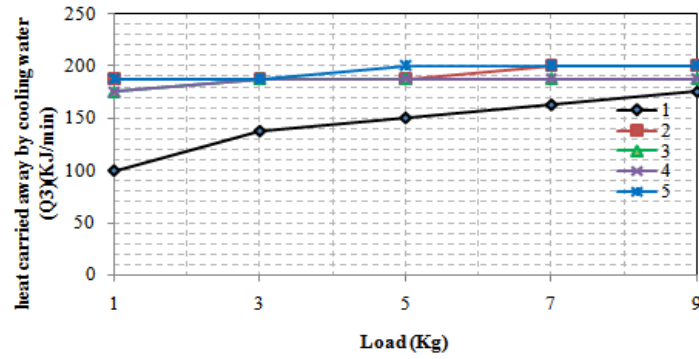**Fig. 3 - Comparative analysis of heat input (Q1) with different load**

Fig. 4 - Comparative analysis of heat carried away by cooling water (Q3) with different load

5.2 Comparative analysis of CI engine Heat balance sheet 2

In this experiment, we analyze the performance of CI engine heat balance with respect to different loads such as 1, 3, 5, 7 and 9 kg. Tables 7 to 10 describe the comparative analysis of the CI engine Heat balance sheet with respect to varying bar pressures 1, 2, 3, 4 and 5, respectively.

Fig. **3** describes the comparative heat input (Q1) analysis with different bar pressures 1, 2, 3, 4 and 5. The heat input (Q1) of bar-1 pressure is 5.781%, 8.74%, 13.043%, and 71.438% higher than the bar-2, bar-3, bar-4, and bar-5 pressure respectively. The variation of heat input with the load is shown in this plot; from this plot, heat input for all the loads decreases gradually from normal cases to 5 bar inlet pressure of air.
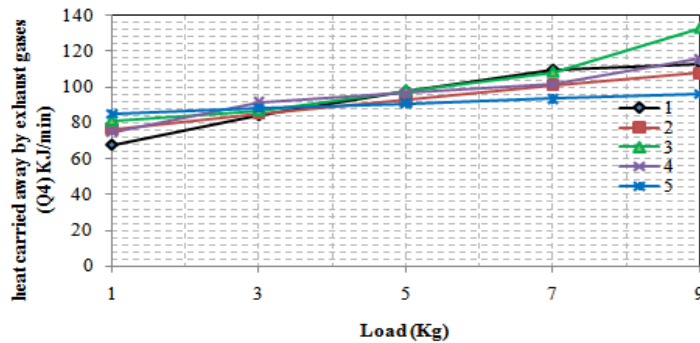

Fig. 5 - Comparative analysis of heat carried away by exhaust gases (Q4) with different load
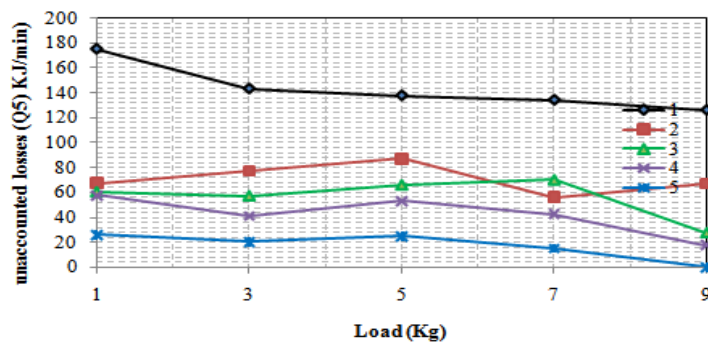

Fig. 6 - Comparative analysis of unaccounted losses (Q5) with different load

Table 6 - Experimental results with heat balance sheet-1 and 1-bar

S. No.	Description	Units	Trail				
			1	**2**	**3**	**4**	**5**
1.	Load applied	(N)	1	3	5	7	9
2.	Torque	(Nm)	1.471	4.4145	7.3575	10.30	13.243

S. No.	Description	Units					
3.	Total fuel consumption	(Kg/hr)	0.4707	0.5369	0.6000	0.665	0.7116
4.	Heat input (Q1)	(KJ/min)	356.94	407.07	455	504.29	539.63
5.	Brake power(Q2)	(KJ/min)	13.566	41.628	69.07	97.07	124.81
6.	Heat carried away by cooling water (Q3)	(KJ/min)	100.23	137.94	150.48	163.02	175.50
7.	Heat carried away by exhaust gases (Q4)	(KJ/min)	67.76	84.18	97.65	109.63	113.15
8.	Unaccounted Losses (Q5)	(KJ/min)	175.08	143.32	137.8	134.27	126.17

Table 7 - Experimental results with heat balance sheet-2 and 2-bar

S. No.	Description	Units	Trail				
			1	2	3	4	5
1.	Load applied	(N)	1	3	5	7	9
2.	Torque	(Nm)	1.4715	4.4145	7.3575	10.30	13.243
3.	Total fuel consumption	(Kg/hr)	0.4567	0.518	0.5773	0.6375	0.6652
4.	Heat input (Q1)	(KJ/min)	346.25	392.66	437.71	455	500.5
5.	Brake power(Q2)	(KJ/min)	13.566	41.628	69.07	97.07	124.81
6.	Heat carried away by cooling water (Q3)	(KJ/min)	188.1	188.1	188.1	200.64	200.64
7.	Heat carried away by exhaust gases (Q4)	(KJ/min)	76.68	85.40	92.88	101.1	107.78
8.	Unaccounted Losses (Q5)	(KJ/min)	67.6	77.53	87.66	56.19	67.27

Table 8 - Experimental results with heat balance sheet-3 and 3-bar

S. No.	Description	Units	Trail				
			1	2	3	4	5
1.	Load applied	(N)	1	3	5	7	9
2.	Torque	(Nm)	1.4715	4.4145	7.3575	10.30	13.243
3.	Total fuel consumption	(Kg/hr)	0.4373	0.4935	0.5563	0.612	0.6244
4.	Heat input (Q1)	(KJ/min)	331.46	374.23	421.86	464.1	473.5
5.	Brake power(Q2)	(KJ/min)	13.566	41.628	69.07	97.07	124.81
6.	Heat carried away by cooling water (Q3)	(KJ/min)	175.56	188.1	188.1	188.1	188.1
7.	Heat carried away by exhaust gases (Q4)	(KJ/min)	81.29	87.03	98.35	108.44	132.93
8.	Unaccounted Losses (Q5)	(KJ/min)	60.74	57.47	66.34	70.49	27.66

Table 9 - Experimental results with heat balance sheet-4 and 4-bar

S. No.	Description	Units	Trail				
			1	2	3	4	5
1.	Load applied	(N)	1	3	5	7	9
2.	Torque	(Nm)	1.4715	4.4145	7.3575	10.30	13.243
3.	Total fuel consumption	(Kg/hr)	0.425	0.4781	0.5368	0.5666	0.5884
4.	Heat input (Q1)	(KJ/min)	322.29	362.55	407.07	429.67	446.20
5.	Brake power(Q2)	(KJ/min)	13.866	41.628	69.07	97.07	124.81
6.	Heat carried away by cooling water (Q3)	(KJ/min)	175.50	188.1	188.1	188.1	188.1
7.	Heat carried away by exhaust gases (Q4)	(KJ/min)	74.87	91.65	96.57	101.82	115.81
8.	Unaccounted Losses (Q5)	(KJ/min)	58.054	41.172	53.33	42.68	17.48

Table 10 - Experimental results with heat balance sheet-5 and 5-bar

S. No.	Description	Units	Trail				
			1	2	3	4	5
1.	Load applied	(N)	1	3	5	7	9
2.	Torque	(Nm)	1.4715	4.4145	7.3575	10.30	13.243
3.	Total fuel consumption	(Kg/hr)	0.4135	0.4567	0.51	0.5368	0.5563
4.	Heat input (Q1)	(KJ/min)	313.49	41.628	69.342	97.07	124.81
5.	Brake power(Q2)	(KJ/min)	13.866	41.628	69.07	97.07	124.81
6.	Heat carried away by cooling water (Q3)	(KJ/min)	188.1	188.1	200.64	200.64	200.64
7.	Heat carried away by exhaust gases (Q4)	(KJ/min)	85.06	88.18	90.93	93.58	96.21
8.	Unaccounted Losses (Q5)	(KJ/min)	26.47	20.34	25.34	15.48	0.2

Fig. **4** describes the comparative analysis of heat carried away by cooling water (Q3) with different bar pressures 1, 2, 3, 4 and 5. The heat carried away by cooling water (Q3) of bar-1 pressure is 12.34%, 15.67%, 19.34%, and 23.12% higher than the bar-2, bar-3, bar-4, and bar-5 pressure respectively. The variation of heat utilized to break power with the load is shown in this plot; from the graph, heat utilized to break power for all the loads increases gradually from normal cases to 5 bar inlet pressure of air.

Fig. **5** describes the comparative analysis of heat carried away by exhaust gases (Q4) with different bar pressures 1, 2, 3, 4 and 5. The heat carried away by exhaust gases (Q4) of bar-1 pressure is 1.806%, 2.551%, 2.768%, and 3.897% higher than the bar-2, bar-3, bar-4, and bar-5 pressure respectively. The variation of heat utilized to break power with the load is shown in this plot; from the graph, heat utilized to break power for all the loads increases gradually from normal cases to 5 bar inlet pressure of air. The variation of heat carried away by cooling water with the load is shown in this plot; from this plot, heat carried away cooling water for all the loads increases gradually from normal cases to 5 bar inlet pressure of air.

Fig. **6** describes the comparative analysis of unaccounted losses (Q5) with the different bar pressures 1, 2, 3, 4 and 5. The unaccounted losses (Q5) of bar-1 pressure are 50.289%, 60.552%, 70.318%, and 87.744% higher than the bar-2, bar-3, bar-4, and bar-5 pressure respectively. The variation of heat utilized to break power with the load, as shown in this plot, from the graph heat utilized to break power for all the loads increases gradually from normal cases to 5 bar inlet pressure of air. The variation of heat carried away by cooling water with the load is shown in this plot; from this

plot, heat carried away cooling water for all the loads increases gradually from normal cases to 5 bar inlet pressure of air.

6. Conclusions

An engine's performance parameters and heat distribution are calculated by varying the inlet pressure of air and compared with the normal pressure of inlet air. By comparing all the results higher value of inlet pressure of air is giving better performance, and the results are listed as follows:

  i.   The performance of the engine was improved due to reduced delay in ignition.
  ii.   The specific fuel consumption for a higher value of inlet pressure shows the best result when compared to the normal atmospheric pressure of inlet air over the entire load range.
  iii. The efficiencies such as thermal brake efficiency indicated thermal Efficiency and mechanical efficiency values for a higher value of inlet pressure of air are more than compared to normal atmospheric pressure of inlet air; and
  iv.   The heat supplied to the engine at the higher-pressure inlet air is less than the atmospheric inlet air pressure.

Acknowledgement

References

[1] Tesfa, B., Mishra, R., Zhang, C., Gu, F. and Ball, A.D. (2013). Combustion and performance characteristics of CI (compression ignition) engine running with biodiesel. Energy, 51,101-115. https://doi:10.1016/j.energy.2013.01.010

[2] Bari, S. and Saad, I. (2015). Performance and emissions of a compression ignition (CI) engine run with biodiesel using guide vanes at varied vane angles. Fuel, 143, 217-228. https://doi.org/10.1016/j.fuel.2014.11.050

[3] Bari, S. and Saad, I. (2014) Effect of guide vane height on the performance and emissions of a compression ignition (CI) engine run with biodiesel through simulation and experiment. Applied Energy, 136, 431-444. https://doi:10.1016/j.apenergy.2014.09.051

[4] Azoumah, Y., Blin, J. and Daho, T. (2006). Exergy efficiency applied for the performance optimization of a direct injection compression ignition (CI) engine using biofuels. Renewable Energy, 34(6), 1494-1500. https://doi:10.1016/j.renene.2008.10.026

[5] Hossain, A.K. and Davies, P.A. (2012). Performance, emission and combustion characteristics of an indirect injection (IDI) multi-cylinder compression ignition (CI) engine operating on neat jatropha and karanji oils preheated by jacket water. Biomass and Bioenergy, 46, 332-342. https://doi:10.1016/j.biombioe.2012.08.007

[6] Szwaja, S. and Grab-Rogalinski, K. (2009). Hydrogen combustion in a compression ignition diesel engine. International journal of hydrogen energy, 34(10), 4413-4421. https:// doi: 10.1016/j.ijhydene.2009.03.020

[7] Dec, J.E. (2009). Advanced compression-ignition engines—understanding the in-cylinder processes. Proceedings of the combustion institute, 32(2), 2727-2742. https://doi.org/10.1016/j.proci.2008.08.008

[8] Bezaire, N., Wadumesthrige, K., Ng, K.S. and Salley, S.O. (2010). Limitations of the use of cetane index for alternative compression ignition engine fuels. Fuel, 89(12), 3807-3813. https://doi:10.1016/j.fuel.2010.07.013

[9] Korakianitis, T., Namasivayam, A.M. and Crookes, R.J. (2011). Diesel and Rapeseed Methyl Ester (RME) pilot fuels for hydrogen and natural gas dual-fuel combustion in compression-ignition engines. Fuel, 90(7), 2384-2395. https://doi:10.1016/j.fuel.2011.03.005

[10] Bika, A.S., Franklin, L. and Kittelson, D.B. (2012). Homogeneous charge compression ignition engine operating on synthesis gas. international journal of hydrogen energy, 37(11), 9402-9411. https:// doi:10.4271/2011-01-0672

[11] Adnan, R., Masjuki, H.H. and Mahlia, T.M.I. (2012). Performance and emission analysis of hydrogen-fueled compression ignition engine with variable water injection timing. Energy, 43(1), 416-426. https://doi: 10.1016/j.energy.2012.03.073

[12] Surawski, N.C., Ristovski, Z.D., Brown, R.J. and Situ, R. (2012). Gaseous and particle emissions from an ethanol fumigated compression ignition engine. Energy Conversion and Management, 54(1), 145-151. https://doi:10.1016/j.enconman.2011.10.011

[13] Moorthi, M., Murugesan, A. and Alagumalai, A. (2022). Effect of nanoparticles on DI-CI engine characteristics fueled with biodiesel-diesel blends—A critical review. Journal of Thermal Analysis and Calorimetry, 1-17. https://doi:10.1007/s10973-022-11234-6

[14] Senthilkumar, P.B., Parthasarathy, M., Nagarajan, R., Murgunachiappan, N., Elumalai, P.V. and Varaprasad, B.H. (2022). The effect of thermal degradation and thermogravimetric analysis on pyrolysis oil production from waste milk packet for CI engine application. Journal of Thermal Analysis and Calorimetry, 1-15. https:// doi:10.1007/s10973-022-11318-3

[15] Bitire, S.O. and Jen, T.C. (2022). Performance and emission analysis of a CI engine fueled with parsley biodiesel-diesel blend. Materials for Renewable and Sustainable Energy, 2022, 1-11. https://doi.org/10.1007/s40243-022-00213-4

[16] Kolli, V.K. and Mandal, P. (2022). Experimental exploration of additive NGQD as a performance and emissions improver of the CI engine with biodiesel-diesel blends. International Journal of Environmental Science and Technology, 19(7), 6705-6720. https:// doi:10.1007/s13762-021-03463-3

[17] Pattanaik, B.P. and Misra, R.D. (2018). Experimental studies on production of deoxygenated vegetable oils and their performance evaluation in a compression ignition engine. Biomass Conversion and Biorefinery, 8(4), 899-908. https://DOI:10.1007/s13399-018-0328-4

[18] Varuvel, E.G., Sonthalia, A., Subramanian, T. and Aloui, F. (2018). NOx-smoke trade-off characteristics of minor vegetable oil blends synergy with oxygenate in a commercial CI engine. Environmental Science and Pollution Research, 25(35), 35715-35724. https://DOI: 10.1007/s11356-018-3484-y

[19] Bragadeshwaran, A., Kasianantham, N., Ballusamy, S., Tarun, K.R., Dharmaraj, A.P. and Kaisan, M.U. (2018). Experimental study of methyl tert-butyl ether as an oxygenated additive in diesel and Calophylluminophyllum methyl ester blended fuel in CI engine. Environmental Science and Pollution Research, 25(33), 33573-33590. https://doi: 10.1007/s11356-018-3318-y

[20] Sahoo, B.B. (2022). Determination of optimum diesel: jatropha blend for compression ignition diesel engines through fuel properties analysis. SN Applied Sciences, 2(12), 1-6. https:// doi:10.1007/s42452-020-03807-7

[21] Cha, J., Yoon, S., Lee, S. and Park, S. (2015). Effects of intake oxygen mole fraction on the near-stoichiometric combustion and emission characteristics of a CI (compression ignition) engine. Energy, 80, 677-686. https:// doi: 10.1016/j.energy.2014.12.023

[22] Kasiraman, G., Geo, V.E. and Nagalingam, B. (2016). Assessment of cashew nut shell oil as an alternate fuel for CI (Compression ignition) engines. Energy, 101, 402-410. https://doi.org/10.1016/j.energy.2016.01.086

[23] Xiao, J., Jia, M., Chang, Y., Li, Y., Xu, Z., Xu, G., Liu, H. and Wang, T. (2018). Numerical optimization and comparative study of n-butanol concentration stratification combustion and n-butanol/diesel reactivity stratification combustion for advanced compression ignition (CI) engine. Fuel, 213, 83-97. https://doi:10.1016/j.fuel.2017.10.104

[24] Lee, T.K., Park, H., Hyun, J., Lee, C. and Song, H.H. (2019). Applicability of high-pressure direct-injected methane jet for a pure compression-ignition engine operation. Fuel, 251, 428-437. https://doi.org/10.1016/j.fuel.2019.04.067

[25] Bhuiya, M., Rasul, M., Khan, M. and Ashwath, N. (2019). Performance and emission characteristics of a Compression Ignition (CI) engine operated with beauty leaf biodiesel. Energy Procedia, 160, 641-647. https://doi:10.1016/j.egypro.2019.02.216

[26] Hamid, M.F., Abdullah, M.K., Idroas, M.Y., Alauddin, Z.Z., Sharzali, C.M., Khimi, S.R. and Sa'ad, S. (2019). Effect of vane numbers on the in-cylinder air flow characteristic in compression ignition (CI) engine run with emulsified biofuel. Materials Today: Proceedings, 17, 989-994. https://doi:10.1016/j.matpr.2019.06.495

[27] Olanrewaju, F.O., Li, H., Andrews, G.E. and Phylaktou, H.N. (2020). Improved model for the analysis of the Heat Release Rate (HRR) in Compression Ignition (CI) engines. Journal of the Energy Institute, 93(5), 1901-1913. https://doi:10.1016/j.joei.2020.04.005

[28] Akintunde, S.B., Obayopo, S.O., Adekunle, A.S., Obisesan, O.R. and Olaoye, O.S. (2021). Combustion and emission study of sandbox seed oil biodiesel performance in a compression ignition (CI) engine. Energy Reports, 7, 3869-3876. https://doi:10.1016/j.egyr.2021.06.070

[29] Oni, B.A., Sanni, S.E. and Olabode, O.S. (2021). Production of fuel-blends from waste tyre and plastic by catalytic and integrated pyrolysis for use in compression ignition (CI) engines. Fuel, 297, 120801. https://doi:10.1016/j.fuel.2021.120801